Analysis of Tool Wear, Surface Roughness and Cutting Power in the Turning Process of Compact Graphite Irons with Different Titanium Content

Sílvia do Nascimento Rosa
silviamec@fem.unicamp.br

Anselmo Eduardo Diniz
anselmo@fem.unicamp.br
University of Campinas
Faculty of Mechanical Engineering
Department of Manufacturing Engineering
13083-970 Campinas, SP, Brazil

Cássio Luiz F. Andrade
cassio@tupy.com.br
Tupy Fundições S.A.
89206-900 Joinville, SC, Brazil

Wilson Luiz Guesser
wguesser@tupy.com.br
Tupy Fundições S.A.
89206-900 Joinville, SC, Brazil
University of the State of Santa Catarina
88035-001 Florianópolis, SC, Brazil

Due to its good mechanical properties, the Compacted (Vermicular) graphite cast iron (CGI) has found a lot of applications in the automobilistic field. One of the applications is the production of high power diesel engine blocks that, due to the higher strength compared to the usual gray cast iron, allows the increase of the pressure inside the cylinder and, consequently, production of high level of energy. The result is the better fuel burning what decreases the fuel consumption and the pollutants' emission levels. However, when CGI replaces gray cast iron, the machining processes used to produce the components are more difficult, with lower tool lives and higher power consumption. Moreover, because usually the raw material to produce cast products of CGI is selected from scrap, some residual level of titanium is present. Thus, the goal of this work is to study the influence of the titanium content (in residual levels) in the turning operation performance with carbide tools, using two cutting speeds. The results show that the alloys with the highest titanium content generated the shortest tool life, but the titanium content influenced neither power consumption nor workpiece surface roughness. Attrition/adhesion was the main tool wear mechanisms verified in this work.
Keywords*: compacted graphite iron, turning, tool wear, roughness, cutting power*

Introduction

Compact Graphite Iron (CGI) has been known for at least six decades, but due to the difficulty to keep magnesium (which is the main responsible for creating the CGI shape of the graphites) in the suitable levels, its production was just carried out in laboratories. The main problems for the production of these alloys were the fact that, because the raw material used to come from scrap, its composition varied from batch to batch, and the control of magnesium content was difficult, since it evaporated during its melting. Just in the beginning of the nineties companies started to look for methods to produce the CGI in industrial scale. The main finding which made it possible was a method to control the magnesium content during foundry process (Guesser and Guedes, 1997).

Fatigue, which is not caused by the lack of mechanical strength, but by the cracks caused by low plasticity, mainly in high temperatures, is one of the main causes of components failure. The elongation of grey cast iron alloys is usually lower than 1%, what in many situations is not enough. Replacing grey cast iron by other material with higher strength, ductility and toughness, as ductile cast iron, is not always possible due to its poor foundry properties, lower heat conductivity, higher Young modulus and etc. The compact graphite iron is an intermediary material between these two, because its mechanical properties are close to the ductile iron, while its physical properties (expansion, conductivity) and properties at high temperatures (thermal fatigue, thermal shock) are close to the grey iron (Stefanescu et al., 1990). With such properties, CGI has found several applications in the automotive field, like its use in diesel high power engine block. Due to the increase of strength when compared to the grey cast iron, the CGI allows an increase in the cylinder pressure, which generates high energy production and fuel economy (Heck et al., 2007).

Due to its better properties, the machining of CGI is more difficult than the machining of grey cast iron (GCI). Tool life decreases up to 20 times when GCI is replaced by CGI, especially in high cutting speeds and in continuous cutting (Heck et al., 2007). Therefore, the present work aims to analyze the machinability of three CGI alloys. Because the raw material in the CGI production is scrap, it is difficult to maintain the titanium content in low levels. So, it is acceptable up to 0.03% of Ti in the alloy (residual level). This work is an attempt to answer, which is the influence of the variation of CGI Ti level (without leaving the residual level) in tool life, workpiece surface roughness and cutting power in a turning process.

Nomenclature

a_p = *depth of cut*
CGI = *Compact Graphite Iron*
CNC = *Computed Numeric Control*
f = *feed*
GCI = *Grey Cast Iron*
L1 = *alloy one*
L2 = *alloy two*
L3 = *alloy three*
Ti = *titanium*
$VB_{Bmáx}$ = *maximum flank wear*
v_c = *speed of cut*

Compact Graphite Iron - Properties and Machinability

Cast iron is considered a Fe-C-Si ternary alloy, with a minimum of 2% C (Chiaverini, 2005).

Grey cast iron is characterized by graphite lamellas (free carbon) randomly oriented, while in the ductile cast iron, graphite is present in nodule shape. In the CGI, graphite particles are in "verm" forms. These particles are elongated and randomly oriented as in the GCI, but are shorter, thicker and with rounded borders. Besides that, the compact graphites are connected to each other (Fig. 1). This graphite morphology leads to a strong cohesion between the graphite and the iron matrix. The smooth surface of the GCI promotes the starting and growth of cracks and, therefore, makes the

Paper accepted January, 2010. Technical Editor: Paulo Eigi Miyagi

material weak and fragile. On the other hand, the connected graphites of the CGI makes difficult the propagation of cracks and, consequently, the occurrence of fractures, what provides superior mechanical properties to the alloy (Abele, Sahm and Schulz, 2002; Dawson, 2007).

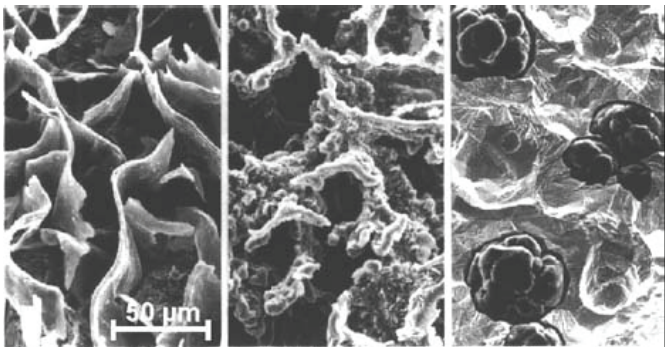

Figure 1. Graphite Morphology in the grey (a) compact (b) and ductile (c) irons (Dawson et al., 2001).

The components and phases present in high percentage in cast iron are mainly graphite, pearlite and ferrite. During solidification the material pass through a temperature range in which austenite shows up and, below 725 ºC, the material becomes ferrite and pearlite. If the cooling process is slow enough and the chemical conditions are suitable, the carbon atoms migrate to form graphite particles. However, if the atoms are not able to leave the matrix, pearlite formation is going to occur, made of an alternate lamellar structure of ferrite and cementite (Fe_3C), which makes the matrix harder and more resistant (Dawson, 2001). The ratio pearlite/ferrite is another determinant factor to the material mechanical resistance. An increase from 15% to 95% of pearlite in the CGI, keeping the other variables constant, leads to an increase in its tensile stress from 300 MPa to 480 MPa, what makes its machining even more difficult (Dawson, 1999).

Mills and Redford (1983, apud Bezerra 2003) cite that when the pearlite interlamellar thickness decreases, tool life also decreases. They compared tool life of a grey cast iron with 2.5% of graphite, with coarse pearlite, with another with thin pearlite and 5% of iron carbide and verified that tool life in the machining of the second alloy was, on average, six times smaller than in the first. Although these results were obtained in a grey cast iron, it can be supposed that the same would occur in a CGI alloy, i.e., tool life will decrease with the increase of the amount of pearlite in a pearlite/ferrite matrix and with the decrease of the pearlite thickness even in a CGI alloy.

Table 1 shows some average properties of the pearlitic grey cast iron, compact graphite iron and ductile iron.

Table 1. Average properties of pearlitic grey cast iron, compact graphite iron and ductile iron (adapted from Dawson, 2001).

Properties	Gray	CGI	Ductile
Tensile Strength (MPa)	250	450	750
Young Modulus (GPa)	105	145	160
Fatigue Resistance (MPa)	110	200	250
Heat Conductivity (W/(mK))	48	37	28
Hardness (HB)	179-202	217-241	217-255
Relative Damping Capacity	1.0	0.35	0.22

All CGI alloys have some nodules of graphites (spheroidic particles). When the nodularity increases, the stiffness also increases and the heat conductivity and machinability decreases. Moreover, with the growth of nodularity the mechanical strength also increases, harming the machinability (Dawson, 2007).

Titanium is present in cast irons as alloying element either to improve the wear resistance (in some grey iron cylinder blocks) or as a residual element, in small amounts (<200 ppm). In this case, the effect of Ti on the microstructure is to form carbides and carbonitrides, very hard particles, and consequently, to reduce machinability. Dawson et al. (2001) carried out some turning experiments with carbide tool and cutting speeds of 150 and 250 m/min and concluded that, when the titanium content in the alloy increases, tool life decreases steeply, mainly for values of Ti content smaller than 0.05%. They stated that the increase of Ti from 0.01 to 0.02% is enough to reduce tool life by roughly 50%.

Materials and Experimental Procedures

The turning experiments were conducted on a CNC lathe with 15 kW of power in the main motor and maximum spindle rotation of 4500 rpm. The cutting power signal was acquired with a sample rate of 100 Hz through the software LabView 8.5 connected to a computer. This measurement was carried out using a resistor shunt placed in parallel with the power control system.

The carbide tool insert used had the ISO code SNMG 120408 in the grade ISO HC-K10, CVD coated with three layers: titanium nitride (TiN), aluminum oxide (Al_2O_3) and titanium carbonitride (TiCN). After the coating process, the TiN layer was removed from the rake face using a micro-sandblasting process, which caused the increase of compressive residual stresses of the insert and, consequently, the increase of its toughness. Therefore, the tool rake face was coated just by two layers: Al_2O_3 e TiCN. The tool holder had the ISO code PSBNR-2525M-12.

The experiment was finished when flank wear height ($VB_{Bmáx}$) reached 0.3 mm. This point was considered the end of tool life. The tool wear measurement was carried out several times during an experiment using an optical microscope with 90x magnification and image analyzer software. After the end of tool life, the cutting edges were taken to a Scanning Electronic Microscope (SEM) with EDS analysis equipment in order to make pictures to subsidize the study of wear mechanisms. Workpiece surface roughness measurements were taken using the R_a and R_y parameters, with a cut-off length of 0.8 mm several times along the experiments.

No cutting fluid was used in the experiments. Feed (f) and depth of cut (a_p) were kept constant in all experiments: f = 0.15 mm/rev, a_p = 1 mm. Two cutting speeds were used, 160 and 250 m/min.

Three different CGI alloys were used. Some of their properties and their Ti content are shown on Table 2. The samples were produced in industrial conditions, with some usual variations in the process from ladle to ladle. These variations resulted in some change in nodularity, inside the usual specification for CGI (0-20% nodularity), in pearlite amount and in pearlite interlamellar spacing. All these variations can affect machinability, so the analysis of the results with different Ti contents must take into account these small variations in the microstructure.

Table 2. Mechanical properties and titanium content of the alloys (data supplied by the manufacturers).

Alloy	Brinell hardness (5/570)		Tensile properties			Pearlite percentage (%)	Pearlite interlamellar spacing (μm)	Nodularity (%)	Ti content (% in weight)
	Surface	Nucleous	UTS (MPa)	YS (MPa)	Elongation (%)				
L1	231	234	517	399	1.92	98	0.45	7	0.007
L2	245	240	490	394	1.13	99	0.30	12	0.03
L3	231	228	513	394	1.50	97	0.35	16	0.03

Samples of the alloys were sandpapered and polished and attacked with Nital. After that, they were taken to a microscope in order to count the number of carbides. In the L1 alloy, 35 carbides were found in an area of 120 mm^2 (0.29 carbonetos/mm^2). They were dispersed in the matrix and mainly placed close to the phosphorus eutectic. In the L2 alloy, 109 carbides were found in an area of 110 mm^2 (0.99 carbonetos/mm^2). They were placed both close to the pearlitic matrix and to the eutectic. In the L3 alloy, 162 carbides were found in an area of 143 mm^2 (1.13 carbonetos/mm^2).

Results and Discussion

The software used to generate the graphics of effects (Figs. 2 to 7) was the Minitab 15. The graphics data represent the average value of two experiments with reliability of 90%.

Figure 2 shows tool lives and their dispersion obtained in turning experiments of L1 and L2 alloys in the cutting speeds of 160 and 250 m/min.

Figure 3 shows Pareto graphic of the effect of the variables in significance order. It can be seen that both factors (cutting speed and kind of alloy) and also their interaction influenced the tool life. However, the kind of alloy was the most significant one.

As can be seen in Fig. 2, the longest tool lives were obtained when the L1 alloy was machined. At v_c = 160 m/min, the tool life for the L1 alloy was, on average, 3.3 times longer than for the L2 alloy and, at v_c = 250 m/min, 1.5 times longer. This result may be related to three factors: titanium content, pearlite thickness and percentage of nodularity.

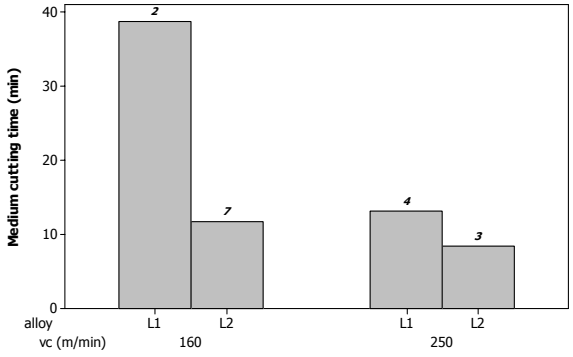

Figure 2. Tool lives for the L1 and L2 alloys.

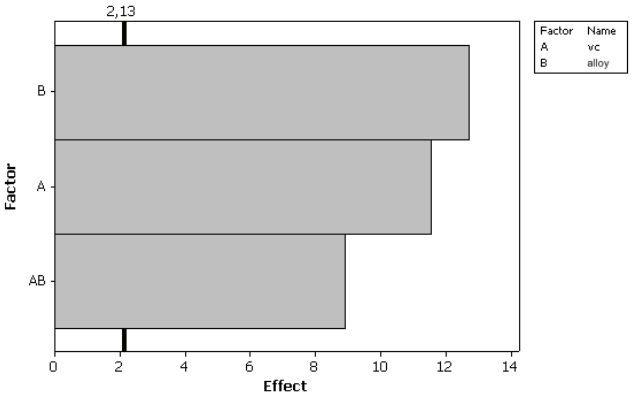

Figure 3. Pareto graphic of variable effects on tool life, for alloys L1 and L2.

Comparing L2 alloy to L1 alloy, titanium content is 4.3 times higher (and consequently the number of carbides is also higher), nodularity is 1.7 times higher and pearlite thickness is 1.5 times smaller (see Table 2). The cut of L2 alloy is more heterogeneous, since the tool hits constantly with different phases (carbides, pearlites and graphites) and the shearing of each phase occurs in a different way, what demands cutting force variation. Moreover, the tendency to occur abrasive wear on the tool is higher due to the higher number of hard particles like the carbides.

Figure 4 shows that the tool lives obtained when the L1 alloy was machined, at both v_c = 160 m/min and v_c = 250 m/min, were longer than when the L3 alloy was machined. It can be seen in Fig. 5 that, again, all the variables (alloy, cutting speed and their interaction) had significant influence on tool life. However, at this time, cutting speed was more influent than the alloy.

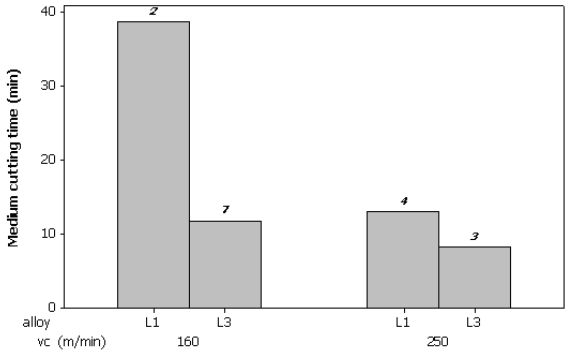

Figure 4. Tool lives for L1 and L3 alloys.

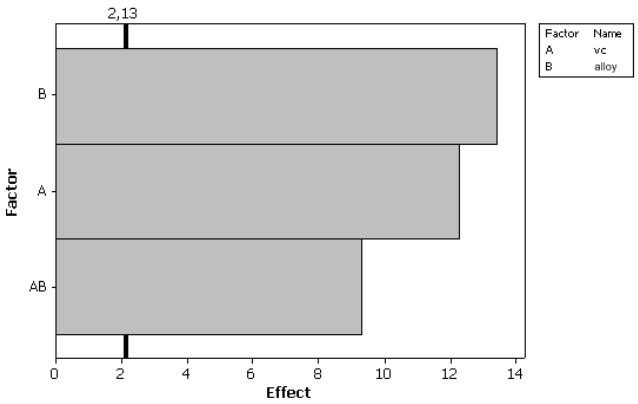

Figure 5. Pareto graphic of variable effects on tool life, for alloys L1 and L3.

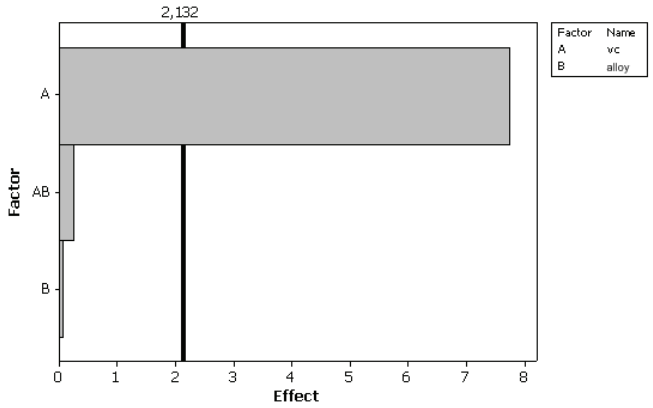

Figure 7. Pareto graphic of the effects, for alloys L2 and L3.

Comparing L3 alloy to L1 alloy, titanium content is 4.3 times higher (and consequently of number of carbides is also higher), nodularity is 2.2 times higher and pearlite thickness is 1.4 times smaller (see Table 2). One or all of these variations were responsible for the shorter tool lives when the L3 alloy was machined. Tool lives for the L3 alloy were, on average, 2.9 times longer than when L1 alloy was machined at 160 m/min and 1.4 longer when L1 alloy was machined at 250 m/min.

Based on the comparisons already done, it can be said that the alloys with the highest titanium content (L2 and L3) present shorter tool lives than the alloy with the smallest Ti content (L1). However, as the two alloys with the highest Ti content presented other variables which could be the cause of the shortening of tool life (pearlite thickness and nodularity), the comparisons between these two alloys (as follows) will determine whether the Ti content is the responsible for the short tool lives or other factors were equally important.

It can be seen in the Fig. 6 that tool lives for L2 and L3 alloys were very similar in both cutting speeds. According to Fig. 7, just the cutting speed was significant for tool life when L2 and L3 are compared. Just the cutting speed had a significant influence on tool life. Tool life was, on average, 1.4 times longer when v_c = 160 m/min was used than when v_c = 250 m/min was used, as can be seen in Fig. 7.

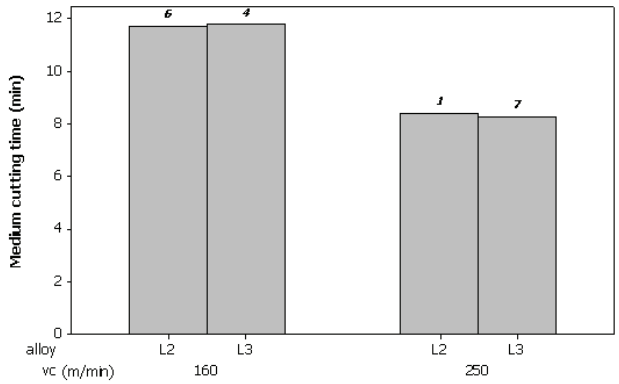

Figure 6. Tool lives for L2 and L3 alloys.

These alloys are just a little different in terms of pearlite thickness, identical in terms of Ti content and very different in terms of nodularity (see Table 2). Therefore, the fact that the alloy is not an influent factor on tool life, when L2 and L3 alloys are compared, leads to the conclusion that when L1 alloy was compared with both, L2 and L3 alloys, it was not the nodularity which caused the strong difference on tool life, but the Ti content and, consequently, the number of carbides Ti formed. In other words, the Ti content was the main cause of tool life variation in these alloys.

As already said by Dawson et al. (2001), the increase of Ti content in CGI decreases tool life and cutting speed has no significant influence. It was also found that in experiments machining CGI with cutting speed of 150 m/min, a percentage of pearlite relatively high influenced tool life. However, with cutting speeds higher than 250 m/min, this variable is not significant anymore (Dawson et al., 2001; Abele, Sahm and Schulz, 2002).

Comparing those results with the results of this work, it can be said that the pearlite percentage was not influent in tool life, because the difference among the alloys was very small. The differences in nodularity could influence tool life results, although they were probably hidden by the variation on Ti content.

Tool Wear Mechanisms

In order to study the wear mechanisms, the cutting edges used in the experiments were taken to a Scanning Electronic Microscope (SEM) equipped with an EDS system. Figures 8, 9 and 10 show the flank wear lands of the carbide cutting edges used to cut with cutting speed of 160 m/min, the L1, L2 and L3 respectively.

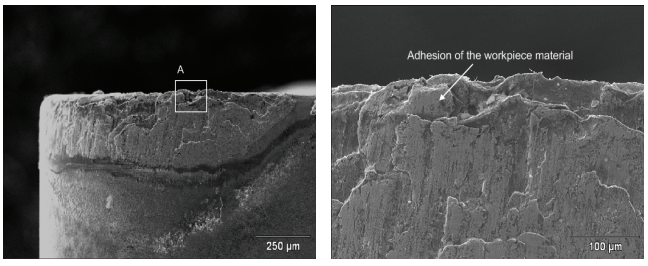

Figure 8. Flank wear land of the cutting edge used to cut L1 alloy at the end of tool life v_c = 160 m/min.

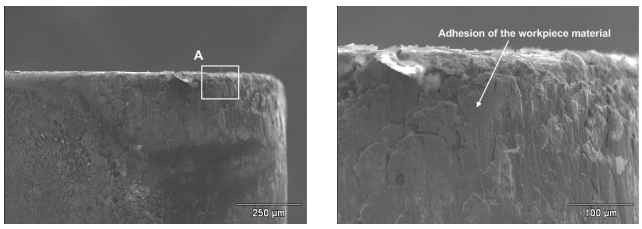

FLANK DETAIL 'A'

Figure 9. Flank wear land of the cutting edge used to cut L2 alloy at the end of tool life v_c = 160 m/min.

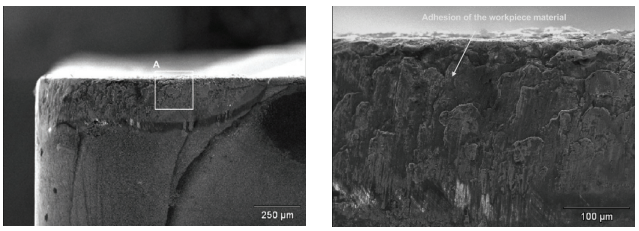

FLANK DETAIL 'A'

Figure 10. Flank wear land of the cutting edge used to cut L3 alloy at the end of tool life v_c = 160 m/min.

The rough appearance of the wear land and the results of EDS analysis showed that the wear lands of the edges used to cut the three alloys were full of workpiece material adhered.

The explanations for the occurrence of such adhesions on the tool flank are the favorable conditions developed during the cutting between the tool flank face and the workpiece. For the adhesion of workpiece/chip material on the tool flank face to occur, some chip material has to be extruded in such a way to be able to pass between the edge and the workpiece and to adhere on the flank wear land. In other words, the material must have some ductility in order to deform and allow the extrusion, and this ductility does not have to be very high (these alloys present elongation smaller than 2% - see Table 1). Trent and Wright (2000) state that for a seizure (adherence) zone to occur on the flank wear land and start the attrition mechanism "attrition", some wear had to have already occurred, generated by some other wear mechanism, like abrasion, for example. Xavier (2003) and Doré (2007) found abrasion wear when cutting CGI alloys with carbide tools. As the alloys with the highest Ti content and highest concentration of carbides were the ones which presented the shortest tool lives, it can be supposed that, at least in the cutting of these alloys, an intense abrasive wear process occurred before the adhesion. This adhesion intensified the wear process because, when the adhered layer was removed by the flow of the workpiece on the flank face, it was removed with its particles of the tool. Trent and Wright (2000) also state that in the presence of vibration, which, of course, was occurring during the cutting, the metal flow past the tool may be very uneven, causing small fragments of the tool to be removed. This mechanism was called attrition by them.

With cutting speed of 250 m/min adhesion was also present, as can be seen in Figs. 11, 12 and 13.

Figures 11, 12 and 13 are very similar to Figs. 8, 9 and 10, i.e., the flank wear lands of the tools used to cut with 250 m/min also were full of workpiece/chip material adhered on it, indicating that attrition was also present in this cutting speed. However, in Fig. 11, related to the tool, which cut the L1 alloy, it can be seen that a large portion of the edge was removed. Probably, the higher amount of heat generated by the process, due to the higher cutting speed, caused the softening of the edge and made easier the removal of large particles of the tool. When the L2 and L3 alloys were cut there was no removal of such large portion of the tool because, due to the shorter tool lives, the cutting edge did not reach the temperature necessary to cause such removal. Moreover, as the life of the tool which cut the L1 alloy was longer, any vibration inherent to the machining process (which, according to Trent and Wright (2000) stimulates the attrition mechanism) could generate a higher number of shocks between workpiece and tool, what led it to mechanical fatigue and, consequently, the chipping of the edge, as can be seen in Fig. 11.

Concluding this item, the main tool wear mechanism when turning the three CGI alloys of this work was attrition regardless the cutting speed used, at least when the tools were close to the end of their lives. For flank wear values smaller than that used to determine the end of tool life (V_B = 0.3 mm), abrasion may have occurred intensely, mainly for the alloys with higher Ti content and higher number of carbides.

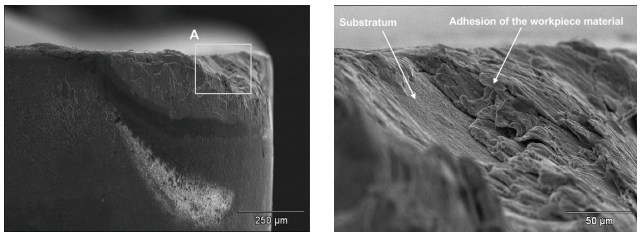

FLANK DETAIL 'A'

Figure 11. Flank wear land of the cutting edge used to cut the L1 alloy at the end of tool life v_c = 250 m/min.

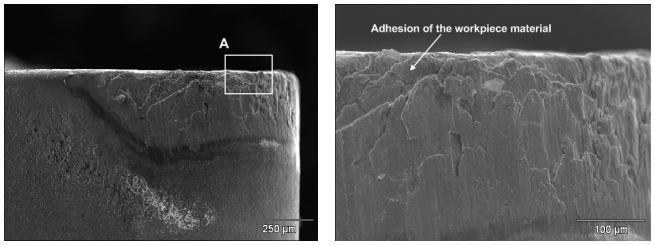

FLANK DETAIL 'A'

Figure 12. Flank wear land of the cutting edge used to cut the L2 alloy at the end of tool life - v_c = 250 m/min.

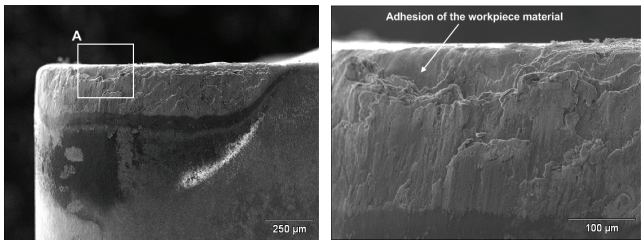

FLANK DETAIL 'A'

Figure 13. Flank wear land of the cutting edge used to cut the L3 alloy at the end of tool life - v_c = 250 m/min.

Workpiece Surface Roughness

The roughness of a machined surface depends on the interaction between two groups of variables: a) cutting conditions, tool geometry and cutting strategies; b) tool wear, vibration of the process, stiffness of the machine tool, workpiece, tool and fixtures, chemical composition and homogeneity of the material. The influence of the variables of the first group can be defined using

equations of theoretical roughness, but the influence of the second group is of difficult estimation (Vivancos et al., 2004).

Figures 14 and 15 show the values of workpiece surface roughness (R_a) along tool lives for all the experiments with v_c = 160 and 250 m/min respectively. The values of maximum roughness (R_y) were also measured and presented a behavior along tool life similar to the R_a behavior.

It can be seen in Fig. 14 that the roughness values in the beginning of tool life were very close (inside the interval from 0.7 to 1.2 mm), regardless the kind of alloy. All the curves presented an initial period of stability after which a steep increase occurred. Of course, the stability period was longer for the L1 alloy curve, since the wear rate was slower for the cutting of this alloy. The sudden change of the curve slope after some cutting time was caused by a supposed variation of tool nose shape generated by tool wear. It is interesting to note that, at the end of tool life, when tool flank wear was 0.3 mm, the values of surface roughness were again close (inside the interval 1.75 to 2.2 mm), regardless the kind of alloy cut. The same behavior of the roughness curves and the same values of roughness at the beginning and at the end of tool life show that the higher presence of Ti content and carbides in the L2 and L3 alloys do not have any direct influence on surface roughness. This fact is another hint to indicate that the tool wear mechanisms for all the alloys were the same and, therefore, the tool nose shapes were similar in all moments of tool life. Of course, due to the faster wear rate of the tools, which machined L2 and L3 alloys, the growth of surface roughness of these materials occurred earlier.

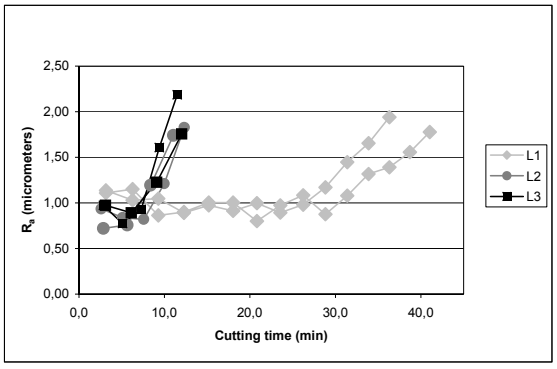

Figure 14. Average roughness (R_a) vs cutting time for v_c = 160 m/min.

For v_c = 250 m/min, the roughness values along tool lives are shown in Fig. 15. Again, the values in the beginning of tool lives were very similar indicating that the kind of alloy did not influence surface roughness. Now the interval which contains all the roughness values for fresh tools is from 0.55 to 0.9 μm, a little lower than this interval for v_c = 160 m/min, indicating that the increase of cutting speed caused the decrease of surface roughness. However, the curve behaviors were the same, i.e., a little stability in the beginning of tool life, followed by an increase of the slopes, which, after that, remained constant up to the end of tool life. Differently of what had occurred with v_c = 160 m/min, the roughness values of the end of tool lives were very different varying from 1.5 μm (for the L1 alloy) to more than 3 μm (for one of the experiments carried out with the L2 alloy). Of course, this difference was caused by differences on the tool nose shape, which is replicated on the surface to form the roughness. But it is interesting to note that the tool that presented the largest variation from its original shape was the one which machined the L1 alloy (see Fig. 11) and the L1 roughness curve was the one which presented the smallest growth along tool life. To explain this fact, it has to be pointed out that the kind of edge chipping shown on Fig. 11 did not occur on the secondary portion of the edge. In a turning process, the secondary cutting edge is responsible for the smoothing of the machined surface and, so, it is responsible for breaking the roughness peaks and decreasing the generated surface roughness. Therefore, the tools used to cut L2 and L3 alloys supposedly presented some variation of the secondary cutting edge, which caused strong increase of surface roughness, shown on Fig. 15. This kind of variation was impossible to be seen in the pictures of the tool taken in this work.

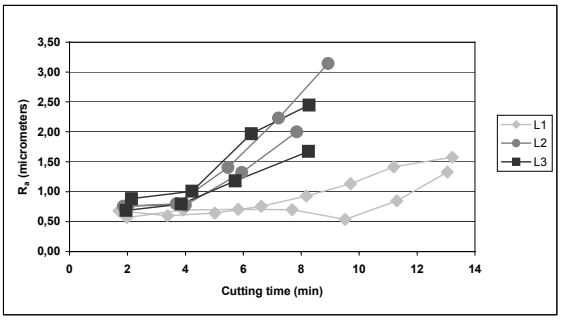

Figure 15. Average roughness (R_a) vs cutting time for v_c = 250 m/min.

Cutting Power

Along the experiments, cutting power was measured in order to check how both the different alloys and the kind of wear influence the consumption of energy. Figure 16 shows cutting power values for each experiment (each bar is an average of the power values of all the experiments made in that condition) carried out with cutting speed of 160 m/min.

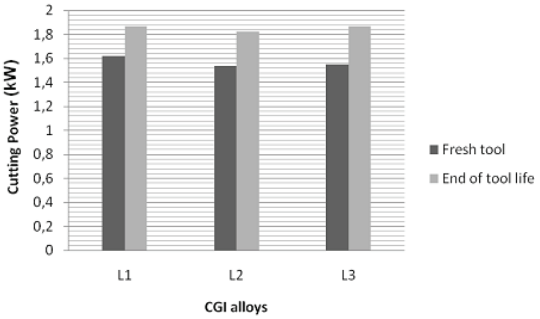

Figure 16. Average cutting power values for all experiments with v_c = 160 m/min.

Some points can be said about cutting power behavior in these experiments:

a) The kind of alloy did not influence cutting power – the higher content of titanium in the L2 and L3 alloys and also their higher nodularity were not significantly important for the cutting power. The titanium content and the number of carbides per area of these alloys, in spite of being much higher than in the L1 alloy, were very low (Ti content maximum of 0.03% and number of carbides per area always below 1.15 carbides/mm^2) and, therefore, not enough to change cutting power. The same is true for the nodularity. Its maximum value was 16%, what was not high enough to bring any change to the cutting power value;

b) The increase of cutting power along tool life was similar in all experiments – the ratio between cutting power in the end of tool life and cutting power in its beginning was between 15 and 20% for all experiments. This small interval of power growth occurred because, as already seen in Figs. 8, 9 and 10, the kind of wear was the same for all experiments (flank wear land full of

workpiece material adhered on it). Therefore, the changing in the friction conditions between workpiece and flank face as flank wear increased was similar for all experiments. Of course, for the L2 and L3 alloys, which presented shorter tool lives, these percentages of increase occurred faster than when the L1 alloy was machined.

Figure 17 shows cutting power values for each experiment (each bar is an average of the power values of all the experiments made in that condition) carried out with cutting speed of 250 m/min. Some things already stated when Fig. 16 was analyzed can also be said here. The kind of alloy did not influence cutting power values due to the same reasons indicated for the analysis of cutting power behavior when v_c = 160 m/min was used (the differences in titanium content, number of carbides and nodularity were not high enough to cause cutting power changes).

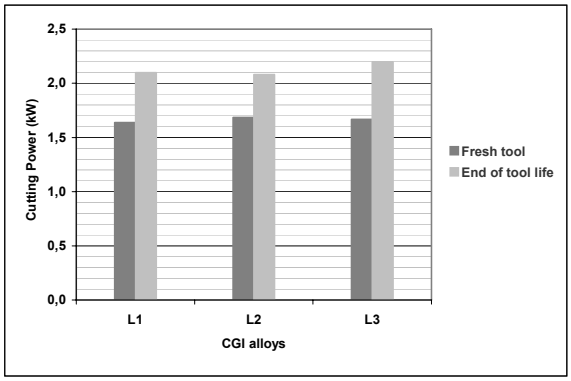

Figure 17. Average cutting power values for all experiments with v_c = 250 m/min.

Again, the increase of cutting power along tool life was similar in all experiments (in the interval of 25 and 31%) since the kind of tool wear was similar for the tools. But interesting points can be stated when the comparison of cutting power obtained with v_c = 160 m/min and v_c = 250 m/min is carried out (comparison of Fig. 16 and 17):

a) In spite of the 56% increase of cutting speed, cutting power in the beginning of tool life increased on average just 6% when cutting speed changed from 160 to 250 m/min. This fact indicates that the increase on cutting speed caused a large decrease of specific cutting force (force per unit of calculated chip area). This decrease of specific cutting power may be generated by both the softening of the workpiece-chip material due to the higher temperature and the decrease in the friction coefficients caused by the higher cutting speed;
b) When v_c = 160 m/min was used, the increase of cutting power along tool life was at maximum 20% and when v_c = 250 m/min was used, this growth reached 31%. This fact indicates that the higher cutting speed caused more damage to the tool shape (not to the height of flank wear, since it never overcame 0.3 mm) and, consequently, caused higher friction between tool-chip and tool-workpiece, what generated this higher increase in cutting power when v_c = 250 m/min was used.

Conclusions

Based on the results here exposed, it can be said that, for the turning of compacted graphite iron in similar conditions to those used in this work:

- increasing titanium content in CGI caused a significant reduction in the tool life even keeping the Ti within levels that can be considered residuals contents;
- titanium content did not influence workpiece roughness values, at least while the tool was in the beginning of life. As the tool life progressed, the titanium content started to influence indirectly roughness growth, once it influenced the rate of the flank wear growth;
- titanium content did not influence cutting power values in the beginning of tool life and also did not influence the rate of cutting power growth along tool life;
- the main tool wear mechanism, regardless of CGI characteristics and the cutting speed, was adhesion/attrition of the worpiece material on the flank surface. Abrasion could have happened before adhesion, but it was not possible to see any trace of it on the flank wear lands.

Acknowledgements

The authors wish to thank Sandvik Coromant for the donation of tools, Tupy S.A. for the donation of workpiece material and CAPES for the financial support.

References

Abele, E., Sahm, A. and Schulz, H., 2002, "Wear mechanism when machining compacted graphite iron", *CIRP Annals*, Vol. 51, No. 1, pp. 53-56.

Bezerra, A.A., 2003, "Study of wear in threading cast iron with high speed", (In Portuguese), Ph.D. Thesis, University of São Paulo, São Carlos, S.P., Brazil, 209 p.

Chaverini, V., 2005, "Steels and Cast Irons", Brazilian Association of Metallurgy and Materials, 7 ed., São Paulo, Brazil, 576 p.

Dawson, S., 1999, "Compacted graphite iron: mechanical and physical properties for engine design", VDI Conference on Materials in Powertrain (Werkstoff und Automobilantrieb), Germany,

Dawson, S., Hollinger, I., Robbins, H., Daeth, J., Reuter, U. and Schulz, H., 2001, "The effect of metallurgical variables on the machinability of compacted graphite iron", SAE World Congress, pp. 1-19.

Dawson, S., 2007, "Compacted graphite iron – a new material for highly stressed cylinder blocks and cylinder hads", Internationales Wiener Motorensymposium, pp. 181-191.

Doré, C., 2007, "Influence of nodularity variation in compacted graphite iron machinability" (In Portuguese), MSc. Thesis, Federal University of Santa Catarina, Florianópolis, SC, Brazil, 132 p.

Guesser, L.W.; Guedes, L.C., 1997, "Recent developments in cast iron applied to the automotive industry" (In Portuguese), IX Symposium on Automotive Engineering, Vol. 8.

Guesser, W.L., Dawson, S. and Schroeder, T., 2001, "Production experience with compacted graphite iron automotive components", American Foundry Society Congress, Vol. 109, pp. 1-11.

Heck, M., Ortner, H.M., Flege, S., Reuter, U. and Ensinger, W., 2007, "Analytical investigations concerning the wear behaviour of cutting tools used for the machining of compacted graphite iron and grey cast iron", *International Journal of Refractory Metals & Hard Materials*, Vol. 26, No. 3, pp. 197-206.

Stefanescu, D.M., Hummer, R. and Nechtelberger, E., 1990, "Compacted Graphite Iron", Metals Handbook, Vol. 15 – Casting, 9 ed. Materials Park: ASM International. pp. 667-677.

Trent, E. and Wright P., 2000, "Metal Cutting", 4th ed. Woburn: Butterworth-Heinemann Publisher, 446p.

Vivancos, J., Luis, C.J., Costa, L. and Ortiz, J.A., 2004, "Optimal machining parameters selection in high speed milling of hardened steels for injection moulds", *Journal of Materials Processing Technology*, Vol. 155-156, No. 1-3, pp. 1505-1512.

Xavier, F.A., 2003, "Technological aspects of turning compacted graphite iron with carbide, ceramic and CBN tools" (In Portuguese), MSc. Thesis, Federal University of Santa Catarina, Florianópolis, SC, Brazil, 146 p.